ORIGINAL ARTICLE

Biogenic Synthesis and Characterization of Zinc Oxide Nanoparticles using *Tecoma stans* Flower Extract and Harnessing its Antimicrobial Potential

Salah Eldeen Dafalla[1,2], Uday M. Muddapur[3], Dinesh Reddy[3], Aparna Shenvi[3], Shivalingsarj V. Desai[3], Ibrahim Ahmed Shaikh[4], Awad Mohammed Al-Qahtani[5], Sunil S. More[6], Aejaz Abdullatif Khan[7], Syed Mohammed Shakeel Iqubal[7], Tasneem Mohammed[7]

[1]Department of Human Anatomy, Ibn Sina National College for Medical Studies, Jeddah, Saudi Arabia, [2]Eastern Sudan College for Medical Sciences and Technology, Port Sudan, Sudan, [3]Department of Biotechnology, KLE Technological University, Hubballi, Karnataka, India, [4]Department of Pharmacology, College of Pharmacy, Najran University, Najran, Saudi Arabia, [5]Department of Family and Community Medicine, College of Medicine, Najran University, Najran, Saudi Arabia, [6]School of Basic and Applied Sciences, Dayananda Sagar University, Bengaluru, Karnataka, India, [7]Department of General Science, Ibn Sina National College for Medical Studies, Jeddah, Saudi Arabia

Abstract

Aims: The present study focuses on the green synthesis of zinc oxide nanoparticles (ZnO NPs) using biocomponents extracted from the *Tecoma stans* flower. Among the extensively studied Nps, ZnO Nps have garnered significant attention due to their versatility in numerous downstream applications. The biomedical industry has witnessed a rapid surge in the utilization of nanotechnology, thanks to the unique and valuable properties offered by Nps. **Materials and Methods:** Fresh flowers were washed and then boiled in distilled water to get the filtrate, which was subjected to centrifugation at 8000 rpm. Next, 20 mL of plant extract was gradually added drop by drop to 80 mL of the 0.1 M zinc acetate solution while continuously stirring the mixture. A white crystalline precipitate formed at 50°C. The size of the nanocrystals was determined through X-ray diffraction (XRD) data using Debye–Scherrer's formula. **Results and Discussion:** An eco-friendly method was employed to synthesize ZnO nanocrystals with an average size ranging from 12 to 44 nm and showed significant antibacterial activity. The synthesized zinc Nps were characterized using scanning electron microscopy and XRD. **Conclusion:** The ZnO Nps obtained exhibited a spherical shape and exhibited antimicrobial activity. These Nps hold great potential for a wide range of applications across various fields, such as biomedical imaging, wastewater treatment, cancer treatment, bioscience, and drug delivery.

Key words: Antimicrobial, nanoparticles, scanning electron microscopy, *Tecoma stans*, X-ray diffraction, zinc oxide

INTRODUCTION

Zinc oxide nanoparticles (ZnO Nps) have gotten a lot of attention in research because of their adaptability in a variety of applications. Compared to those created by other species, plant-made Nps are more stable and varied in form and size.[1] Ranking as the second most abundant metal oxide, ZnO Nps offer affordability, safety, and ease of manufacturing. Notably, ZnO Nps exhibit optical, electrical, and photocatalytic characteristics, making them valuable in fields such as solar cells, photocatalysis, and chemical sensing. In the biomedical realm, ZnO Nps are renowned for their low toxicity and excellent ultraviolet (UV) absorption capabilities, rendering them suitable for applications in areas like medicine. Their rigid structure further enhances

Address for correspondence:
Uday M. Muddapur, Department of Biotechnology, KLE Technological University, BVB Campus, Vidyanagar, Hubballi - 580031, Karnataka, India.
E-mail: muddapur@kletech.ac.in\shakeeliqubal@gmail.com

Received: 30-04-2025
Revised: 14-06-2025
Accepted: 23-06-2025

Graphical Abstract

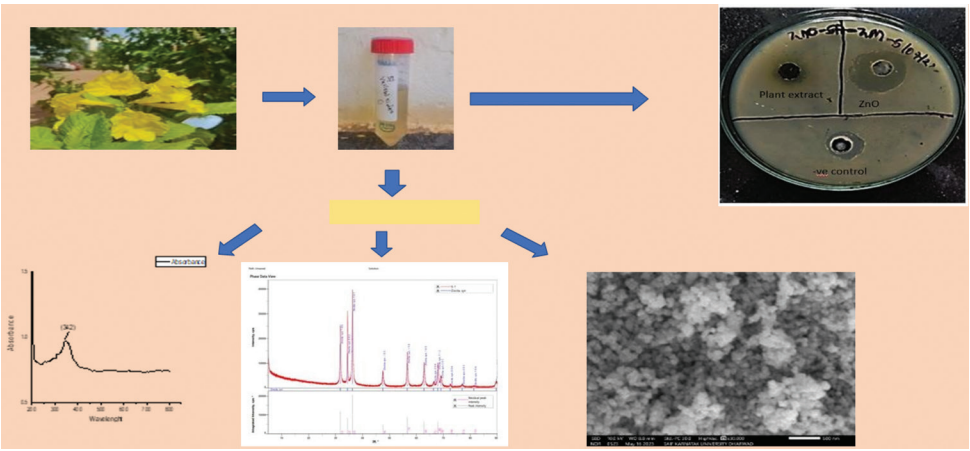

their utility in the ceramic industry. ZnO Nps are produced by all ways including direct precipitation, homogeneous precipitation, solvothermal technique, sonochemical method, reverse micelles, sol-gel method, hydrothermal, thermal breakdown, and microwave irradiation.[2] Its simplicity, environmental friendliness, and wide antibacterial effect are helping the biological method of generating ZnO Nps to become more widespread.[3] One notable advantage of ZnO Nps in biomedicine lies in their favorable surface properties, which naturally resist insecticidal and microbial activity. Consequently, they find extensive use in biological labeling, biological sensing, drug delivery, gene delivery, and nanomedicine. Importantly, ZnO has received approval from the Food and Drug Administration as a safe material.[4,5]

Green synthesis methods are gaining popularity since they eliminate the high costs and use of toxic chemicals as well as harsh conditions for reduction and stabilization.[6] Considering this, biological techniques have been employed to successfully synthesize various metal and metal oxide Nps.[7-10] ZnO NPs have recently been exploited in food packaging materials and matrices, and methods for integrating ZnO into such matrices have been disclosed. ZnO is integrated into the packaging matrix, allowing it to interact with the food ingredients and provide preservation effects.[11] ZnO NPs are currently employed as a component in sunscreens, paints, and coatings due to their transparency to visible light and strong UV absorption.[12] Antibacterial creams, ointments, and lotions, as well as self-cleaning glass, ceramics, and deodorants, all contain them.[13]

Metal Nps are increasingly being used in biomedicine and other fields around the world.[14] Many metal particles found in cosmetics, detergents, toothpaste, soaps, shampoos, pharmaceuticals, and pharmaceutical items encounter humans. Our goal for this broad application is to focus on the synthesis of zinc Nps and antibacterial uses from *Tecoma stans*.

MATERIALS AND METHODS

Steps to make flower extract

After collecting 10 g of fresh flowers from the plant, the flowers were washed once with tap water and then re-washed with distilled water. The flowers were then chopped with a knife and transferred to a 250 mL beaker containing 100 mL of distilled water. The mixture was then boiled for 15 min. The resulting extract was then allowed to cool and then filtered using Whatman filter paper. The filtrate was then subjected to centrifugation at 8000 rpm.

Fabrication of ZnO Nps

A solution of zinc acetate was prepared by dissolving 2.195 g of zinc acetate, which corresponds to a concentration of 0.1 M, in 100 mL of distilled water. To ensure complete solubilization, the mixture was placed on a magnetic stirrer for 1 h. Next, 20 mL of plant extract was gradually added drop by drop to 80 mL of the 0.1 M zinc acetate solution while continuously stirring the mixture. The stirring process should be maintained throughout. Freshly prepared 2M NaOH was then added dropwise to the solution with gentle stirring, adjusting the pH to 10. Afterward, the solution was placed in a water bath at 50°C for 1 h while continuing to stir the reaction mixture using a magnetic stirrer. A white crystalline precipitate formed, which was subsequently washed multiple times using distilled water until a pH of 7 was achieved.

Evaluation of synthesized ZnO NPs

UV visible spectroscopy analysis of synthesis

The UV-vis spectroscopy analysis was conducted to investigate the absorption characteristics of biologically synthesized ZnO NP using a UV 9600A UV/visible spectrophotometer. The purpose of the analysis was to identify the absorption

maxima of the ZnO NP within the wavelength range of 300–600 nm. By plotting the wavelength on the X-axis and the corresponding absorbance on the Y-axis, a graph was generated to visualize the absorption behavior of the ZnO NP.

Fourier transform infrared spectroscopy (FTIR) analysis of synthesized ZnO Nps

FTIR analysis was used to identify potential functional groups in the biomolecules found in the plant extract. The goal of this study was to see if the biomolecules were successfully capped onto the ZnO NPs. By comparing the FTIR spectra of the capped biomolecules with ZnO NP to that of the extract from leaves alone, the presence of specific functional groups responsible for reduction, stabilization, and capping agents could be confirmed. The FTIR analysis covered a spectral range of 400–4000 cm^{-1}.

Scanning electron microscope (SEM)

SEM is a specialized type of electron microscope that utilizes a focused beam of electrons to generate high-resolution images of a sample's surface. By scanning the surface with this electron beam, interactions occur between the electrons and atoms within the sample, generating diverse signals that provide valuable information about the sample's composition and surface topography. The electron beam moves in a raster scan pattern, and the resulting image is formed by combining the beam's position with the intensity of the detected signal. In the most used mode of operation, secondary electrons emitted from atoms excited by the electron beam are captured using a secondary electron detector known as the Everhart–Thornley detector. The intensity of the detected signal, and thus the number of secondary electrons collected, depends on factors such as the topography of the specimen. Some advanced SEMs can achieve exceptional resolutions surpassing 1 nanometer.

X-ray diffraction (XRD) analysis

A common method in materials science for determining a material's crystallographic structure is XRD analysis. This technique entails subjecting the material to incident X-rays and determining the scattering angles and intensities of the X-rays that the material emits. X-rays are specifically utilized in this process because their wavelength λ typically falls within a similar range (1–100 angstroms) as the spacing d between crystal planes in the material. By examining the resulting diffraction pattern, valuable insights into the material's crystal structure can be obtained.

RESULTS AND DISCUSSION

Extraction of flower

A total of 10 g of fresh flower extract from *T. stans* were obtained and thoroughly washed. The extract was finely chopped and ground using a mortar and pestle, followed by boiling in 100 mm of distilled water. Subsequently, the extract was filtered and centrifuged, and the resulting supernatant was carefully collected and stored at a temperature of 4°C for future applications. Throughout the process, the color of the extract transitioned from pale yellow to the formation of a light-yellow precipitate [Figure 1].

UV-visible spectral analysis

To verify the reduction of Zn ions in the solution mixture, UV-visible spectroscopy was employed. The spectral data of the synthesized ZnO were recorded in the wavelength range of 200–600 nm, with a focus on electronic transitions. UV-visible spectrophotometry finds extensive use in biochemistry for species determination and the examination of biochemical processes. Figure 2 shows the absorption intensity of the prepared ZnO NPs measured in the wavelength range from 300 to 500 nm. The ZnO NPs prepared using *T. stans* flower extract showed λmax at 342 nm, which is supported by the literature.[15-17]

Effect of pH

The pH levels of a colloidal solution containing flower extract were controlled within the range of 7, 8, and 9. Test

Figure 1: Yellow-colored precipitate

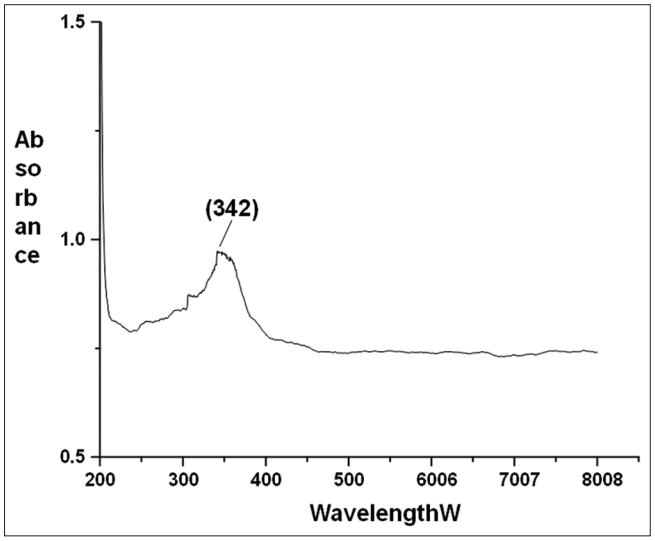

Figure 2: Ultraviolet absorbance of zinc oxide nanoparticle of *Tecoma stans*

tubes were used to hold samples, and the pH was adjusted to 2 using NaOH and HCl. The absorbance of the solution was then measured using a UV-visible spectrophotometer. This process was repeated for pH levels ranging from 7 to 9, and the absorbance values were recorded. The pH level with the highest peak in absorbance was identified, and it was selected as the optimal pH for the bulk synthesis of ZnO NPs. The optimum pH was found to be 8 [Table 1 and Figure 3].

Effect of temperature

The temperature of a colloidal solution containing flower extract was controlled within the range of 30, 40, and 50°C. Test tubes were utilized to hold samples, and the temperature was adjusted to 30°C using an incubator and thermostat. The absorbance was measured. This process was repeated for temperature levels ranging from 30°C to 50°C, and the absorbance values were recorded [Table 2 and Figure 4]. The temperature with the highest peak in absorbance was identified, and it was chosen as the optimal temperature for the bulk synthesis of ZnO NPs. The optimum temperature was found to be 30°C. The temperature with the highest peak in absorbance was identified, and it was chosen as the optimal temperature for the bulk synthesis of ZnO NPs. The optimum temperature was found to be 30°C.

FT-IR spectral analysis

The FTIR spectrum of the synthesized ZnO NPs exhibited distinct absorption bands, indicating the presence of various functional groups associated with Np stabilization and formation [Figure 5]. A broad absorption peak observed at around 3313 cm^{-1} corresponds to the O–H stretching vibration, suggesting the presence of hydroxyl groups, possibly from adsorbed water molecules or phytochemical compounds used in the synthesis. The band at 2122 cm^{-1} is typically associated with C≡C stretching of alkynes. A peak appearing at 1632 cm^{-1} is attributed to the bending vibration of H–O–H (water molecules) or C=O stretching, indicating the presence of carbonyl groups. Peaks at 1399 cm^{-1} and 1253 cm^{-1} may correspond to C–N stretching vibrations of amines and C–O stretching of carboxylic acids or esters, respectively, suggesting the involvement of organic stabilizers or reducing agents. The prominent peak at 1058 cm^{-1} can be assigned to C–O–C stretching vibrations of alcohols or

Table 1: UV-vis for optimum pH of *Tecoma stans*

pH	P/V	Wavelength (nm)	Abs
7	Peak	266.00	4
8	Peak	391.00	3.18
9	Peak	251.00	3.5

UV: Ultraviolet

Table 2: UV-vis for optimum temperature of *Tecoma stans*

Temperature	P/V	Wavelength (nm)	Abs
30°C	Peak	365.00	4
40°C	Peak	470.00	4
50°C	Peak	485.00	3.8

UV: Ultraviolet

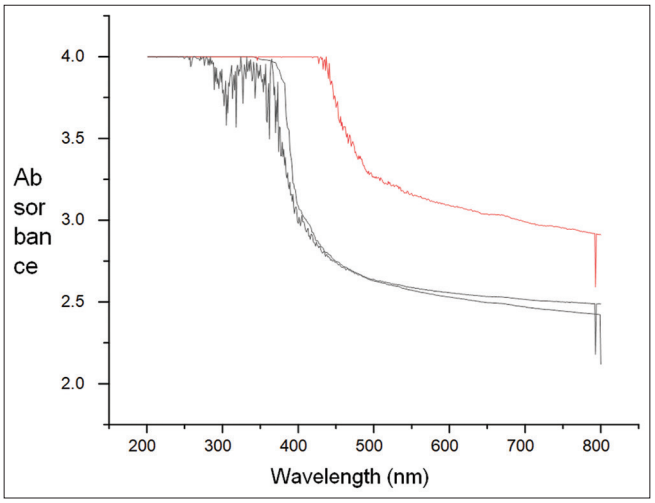

Figure 3: Peak of the spectrum at different pH of *Tecoma stans*

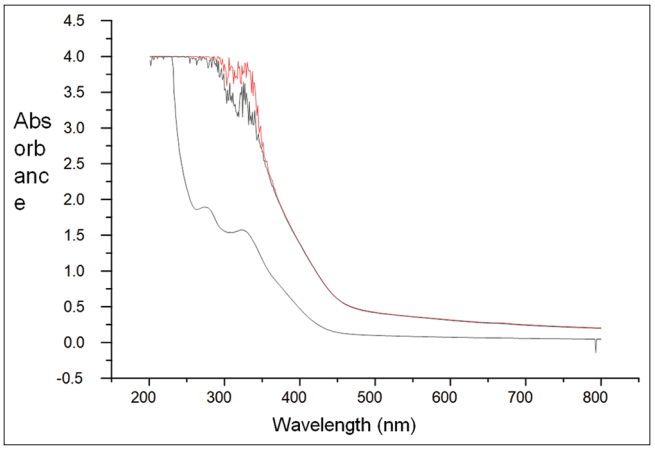

Figure 4: Peak of the spectrum at different temperatures of *Tecoma stans*

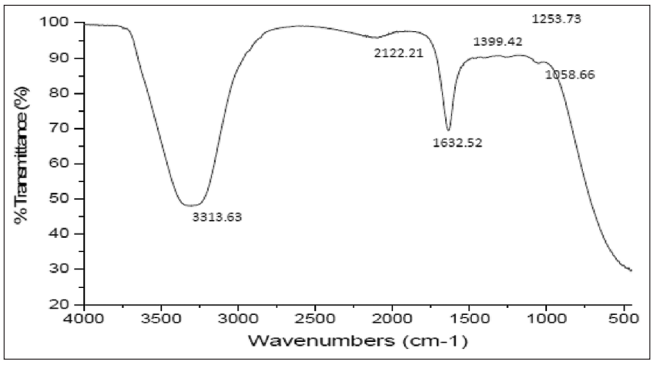

Figure 5: Fourier transform infrared spectroscopy spectrum of zinc oxide nanoparticles produced from flower extracts of *Tecoma stans*

ethers. Furthermore, the characteristic absorption band below 600 cm^{-1}, though not sharply resolved in the image, typically corresponds to Zn–O stretching vibrations, confirming the successful formation of ZnO NPs.[18,19]

SEM analysis

The SEM analysis, specifically shown in Figure 6, provided insights into the shape, structure, and size of the synthesized ZnO NPs. The micrographs obtained from the SEM confirmed that the ZnO NPs possessed a nano-sized range, exhibited a spherical shape, and displayed a uniform distribution.

Furthermore, the SEM results revealed that the choice of precursors had an impact on the size and shape of the Nps. When zinc acetate was utilized as a precursor, the ZnO molecules exhibited a slow growth rate, resulting in the formation of small spherical structures that accumulated in a bullet-like manner.

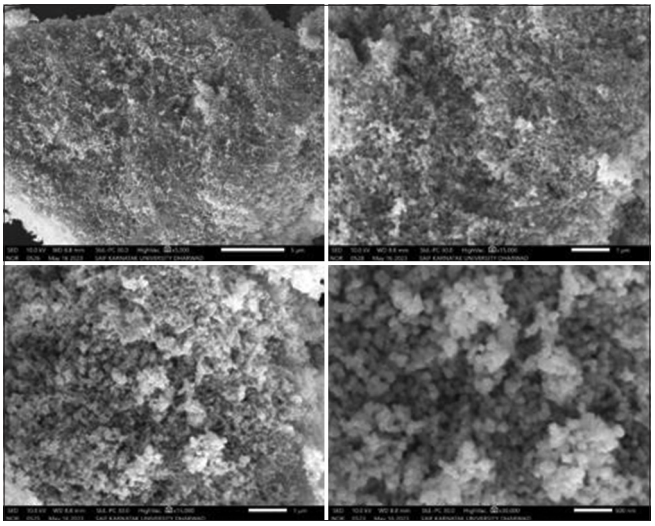

Figure 6: Scanning electron microscope images of zinc oxide nanoparticles of flower extracts of *Tecoma stans* at different magnifications

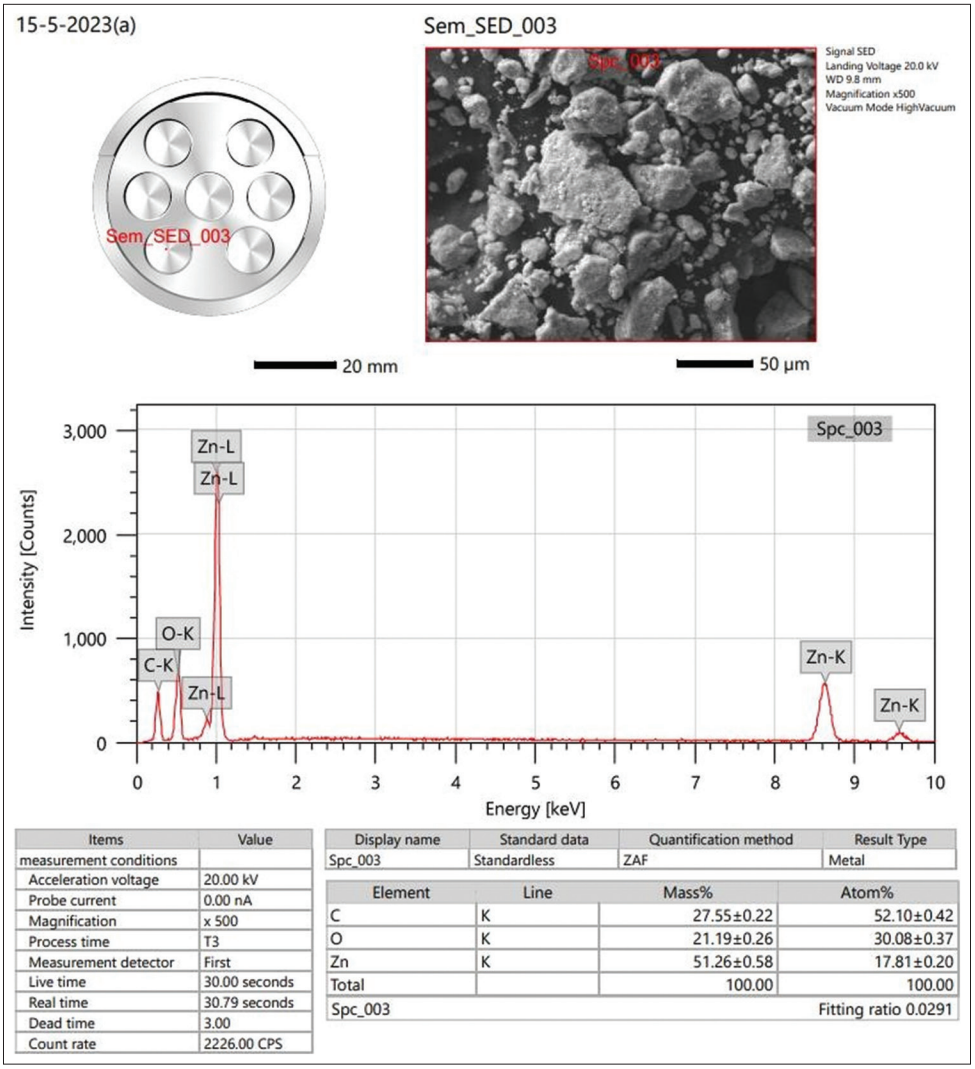

Items	Value
measurement conditions	
Acceleration voltage	20.00 kV
Probe current	0.00 nA
Magnification	x 500
Process time	T3
Measurement detector	First
Live time	30.00 seconds
Real time	30.79 seconds
Dead time	3.00
Count rate	2226.00 CPS

Display name	Standard data	Quantification method	Result Type
Spc_003	Standardless	ZAF	Metal

Element	Line	Mass%	Atom%
C	K	27.55±0.22	52.10±0.42
O	K	21.19±0.26	30.08±0.37
Zn	K	51.26±0.58	17.81±0.20
Total		100.00	100.00
Spc_003			Fitting ratio 0.0291

Figure 7: Energy-dispersive X-ray spectroscopy result of zinc oxide nanoparticles of leaf extracts of *Tecoma stans*

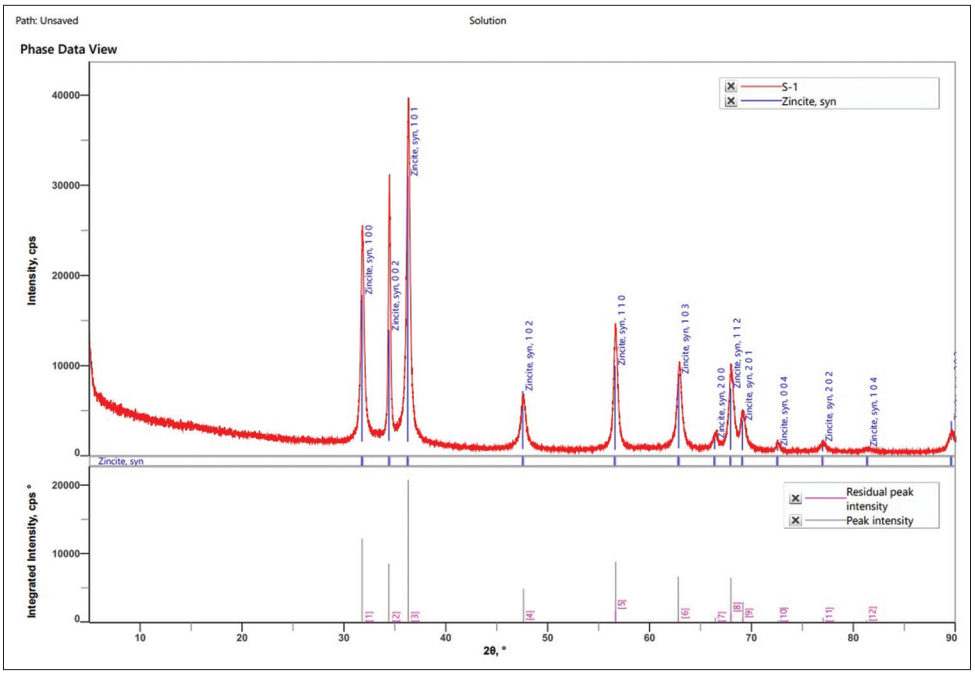

Figure 8: X-ray diffraction plotting of flower extract of *Tecoma stans*

Energy dispersive X-ray (EDS) analysis

The analysis of the EDX spectra [Figure 7] indicated the presence of the necessary phases of Zn, O, and C in the samples, confirming the high purity of the synthesized ZnO NPs. The anticipated stoichiometric mass percentages of Zn, O, and C are theoretically expected to be 51.26%, 21.19%, and 27.55%, respectively.

XRD

The XRD analysis of the synthesized ZNPs clearly demonstrates the presence of a crystalline structure, as evident from the XRD pattern. Distinctive and well-defined diffraction peaks were observed at specific 2θ values shown in Figure 8, Table 3, namely 31.79002, 34.44384, 36.29941, 47.56371, 56.60806, 62.81039, 66.39204, 67.92777, 69.07093, 72.51331, 76.98415, and 81.23695°. These peaks correspond to the diffraction lattice planes indexed as (100), (002), (101), (102), (110), (103), (200), (112), (201), (004),(202) and (104), respectively,[20] confirming the spherical structure of the synthesized Nps. The pattern obtained aligns with the standard peaks provided by the International Centre for Diffraction Data.

To determine the average size of the ZNPs, the Debye–Scherrer's equation was utilized, taking into account the highest intensity peak (104). In this equation, ω represents the X-ray wavelength emitted by Cu-Kα (1.540560 Å), β denotes the full width at half maximum of the diffraction peak in radians, θ represents the Bragg's angle in degrees, and K is the shape factor with a value of 0.9.

Table 3: Calculation of crystalline size of *Tecoma stans* flower extract

S. No.	2θ°	FWHM°	Radian	Crystallite size (nm)
1	31.79002	0.3583	0.005991	26.20
2	34.44384	0.2198	0.003561	44.37
3	36.29941	0.4001	0.006066	26.19
4	47.56371	0.5942	0.009306	17.13
5	56.60806	0.4351	0.006866	24.97
6	62.81039	0.6241	0.008639	20.47
7	66.39204	0.5546	0.008616	20.94
8	67.92777	0.4432	0.007845	23.20
9	69.07093	0.4908	0.008375	21.80
10	72.51331	0.5719	0.005464	34.28
11	76.98415	0.3361	0.01014	19.02
12	81.23695	0.648	0.01609	12.36

$$D = \frac{K\omega}{\beta\cos\theta}$$

The XRD analysis yielded an average Np size of 24.1841 nm.

Antimicrobial activity

Zinc Nps are tiny pieces of ZnO that kills germs and fungi.[21,22] Our results are showing good zone of inhibition against bacteria [Figure 9]. It works by releasing Zn^{2+}, making reactive oxygen species, damaging the cell membrane, and sticking to microbial proteins and nucleic acids. How well the Nps kill germs depends on their size and shape.[22-24]

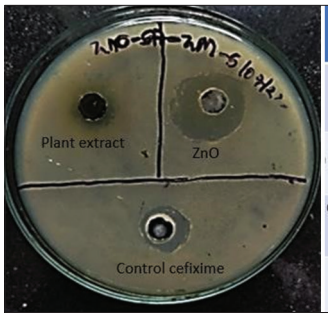

Organism	*E.coli*
Disks	Zone of inhibition
Plant extract	**12mm**
Control (cefixime)	**14mm**
ZnO	**20 mm**

Figure 9: Antimicrobial activity

CONCLUSION

The flower extract of *T. stans* offers a rapid and environmentally friendly method for the biological synthesis of zinc Nps. This approach is simple and effective, eliminating the need for hazardous reducing and stabilizing agents. The resulting ZnO nanocrystals have an average size range of 12–44 nm, as confirmed by analytical studies. In addition, these Nps exhibited significant antimicrobial activity against *Escherichia coli.* The synthesis of ZnO Nps is currently at an early stage, necessitating further research to understand the mechanism behind their formation. A deeper understanding holds the potential for refining the synthesis process, allowing for precise control over the size and shape of the Nps. Therefore, more focused studies are needed to explore and optimize the parameters that govern Np formation, including their potential biomedical applications.

ACKNOWLEDGMENTS

The authors are thankful to KLE Tech. University, Hubballi, India and ISNC, Jeddah, Saudi Arabia.

AUTHOR CONTRIBUTIONS

All authors contributed equally toward this research.

REFERENCES

1. El Shafey AM. Green synthesis of metal and metal oxide nanoparticles from plant leaf extracts and their applications: A review. Green Process Synth 2020;9:304-39.
2. Droepenu EK, Wee BS, Chin SF, Kok KY, Maligan MF. Zinc oxide nanoparticles synthesis methods and its effect on morphology: A review. Biointerface Res Appl Chem 2022;12:4261-92.
3. Gunalan S, Sivaraj R, Rajendran V. Green synthesized ZnO nanoparticles against bacterial and fungal pathogens. Prog Nat Sci Mater Int 2012;22:693-700.
4. Singh TA, Das J, Sil PC. Zinc oxide nanoparticles: A comprehensive review on its synthesis, anticancer and drug delivery applications as well as health risks. Adv Colloid Interface Sci 2020;286:102317.
5. Hamdy E, Al-Askar AA, El-Gendi H, Khamis WM, Behiry SI, Valentini F, *et al*. Zinc oxide nanoparticles biosynthesized by *Eriobotrya japonica* leaf extract: Characterization, insecticidal and antibacterial properties. Plants 2023;12:2826.
6. Madani M, Hosny S, Alshangiti DM, Nady N, Alkhursani SA, Alkhaldi H, *et al*. Green synthesis of nanoparticles for varied applications: Green renewable resources and energy-efficient synthetic routes. Nanotechnol Rev 2022;11:731-59.
7. Husen A, Siddiqi KS. Phytosynthesis of nanoparticles: Concept, controversy and application. Nanoscale Res Lett 2014;9:229.
8. Jeevanandam J, Chan YS, Danquah MK. Biosynthesis of metal and metal oxide nanoparticles. ChemBioEng Rev 2016;3:55-67.
9. Muddapur UM, Alshehri S, Ghoneim MM, Mahnashi MH, Alshahrani MA, Khan AA, *et al*. Plant-based synthesis of gold nanoparticles and theranostic applications: A review. Molecules 2022;27:1391.
10. Moalwi A, Kamat K, Muddapur UM, Aldoah B, AlWadai HH, Alamri AM, *et al*. Green synthesis of zinc oxide nanoparticles from *Wodyetia bifurcata* fruit peel extract: Multifaceted potential in wound healing, antimicrobial, antioxidant, and anticancer applications. Front Pharmacol 2024;15:1435222.
11. Espitia PJ, Soares ND, Coimbra JS, De Andrade NJ, Cruz RS, Medeiros EA. Zinc oxide nanoparticles: Synthesis, antimicrobial activity and food packaging applications. Food Bioprocess Technol 2012;5:1447-64.
12. Franklin NM, Rogers NJ, Apte SC, Batley GE, Gadd GE, Casey PS. Comparative toxicity of nanoparticulate ZnO, bulk ZnO, and ZnCl2 to a freshwater microalga (*Pseudokirchneriella subcapitata*): The importance of particle solubility. Environ Sci Technol 2007;41:8484-90.
13. Bwatanglang IB, Obulapuram PK, Mohammad F, Albalawi AN, Chavali M, Al-Lohedan HA, *et al*. Metal oxide-involved photocatalytic technology in cosmetics and beauty products. In: Metal Oxides for Optoelectronics and Optics-Based Medical Applications. Netherlands: Elsevier; 2022. p. 301-37.
14. Yaqoob AA, Ahmad H, Parveen T, Ahmad A, Oves M, Ismail IM, *et al*. Recent advances in metal decorated nanomaterials and their various biological applications: A review. Front Chem 2020;8:341.
15. Balouiri M, Sadiki M, Ibnsouda SK. Methods for in vitro evaluating antimicrobial activity: A review. J Pharm Anal 2016;6:71-9.
16. Rupa SA, Moni MR, Patwary MA, Mahmud MM, Haque MA, Uddin J, *et al*. Synthesis of novel tritopic hydrazone ligands: Spectroscopy, biological activity, DFT, and molecular docking studies. Molecules 2022;27:1656.
17. Rahman MM, Islam MB, Biswas M, Khurshid Alam AH. *In vitro* antioxidant and free radical scavenging activity

of different parts of *Tabebuia pallida* growing in Bangladesh. BMC Res Notes 2015;8:621.
18. Mousa M, Khairy M. Synthesis of nano-zinc oxide with different morphologies and its application on fabrics for UV protection and microbe-resistant defense clothing. Textile Res J 2020;90:2492-503.
19. Getie S, Belay A, Chandra Reddy AR, Belay Z. Synthesis and characterizations of zinc oxide nanoparticles for antibacterial applications. J Nanomed Nanotechnol 2017;8:1-8.
20. Al Awadh AA, Shet AR, Patil LR, Shaikh IA, Alshahrani MM, Nadaf R, *et al*. Sustainable synthesis and characterization of zinc oxide nanoparticles using *Raphanus sativus* extract and its biomedical applications. Crystals 2022;12:1142.
21. Gudkov SV, Burmistrov DE, Serov DA, Rebezov MB, Semenova AA, Lisitsyn AB. A mini review of antibacterial properties of ZnO nanoparticles. Front Phys 2021;9:641481.
22. Meruvu H, Vangalapati M, Chippada SC, Bammidi SR. Synthesis and characterization of zinc oxide nanoparticles and its antimicrobial activity against *Bacillus subtilis* and *Escherichia coli*. J Rasayan Chem 2011;4:217-22.
23. Dafalla SE, Aldabaan NA, Muddapur UM, Angadi S, Patil LR, Shaikh IA, *et al*. Green and sustainable synthesis of the ZnONPs using leaf extract of *Guazuma ulmifolia* for antioxidant and antimicrobial activities. J Umm Al-Qura Univ Appl Sci 2024;11:308-18.
24. Shaikh IA, Turakani B, Mahnashi MH, Alqahtani AS, Hariri SH, Ghoneim MM, *et al*. Environmentally friendly production, characterization, and evaluation of ZnO NPs from *Bixa orellana* leaf extract and assessment of its antimicrobial activity. J King Saud Univ Sci 2023;35:102957.

Source of Support: Nil. **Conflicts of Interest:** None declared.